Temperature Corrected Strain Measurements Using Optical Time Domain Reflectometry

by

Carl P. Jacobson

Thesis submitted to the Faculty of the
Virginia Polytechnic Institute and State University
in partial fulfillment of the requirements for the degree
of
MASTER OF SCIENCE
in
Electrical Engineering

APPROVED:

Dr. R.O. Claus

Dr. I. Jacobs

Dr. T. C. Poon

May, 1990

Blacksburg, Virginia

TEMPERATURE CORRECTED STRAIN MEASUREMENTS

USING OPTICAL TIME DOMAIN REFLECTOMETRY

by

Carl P. Jacobson

Committee Chairman: Richard O. Claus

Electrical Engineering

(ABSTRACT)

A method of using optical fiber to measure strain and correct for the effects of temperature is proposed. A means of measuring apparent strain is given, pure temperature is measured using Fresnel-backscatter based Optical Time Domain Reflectometry, and a method for combining the two measurements to obtain a measurement of mechanically-induced strain alone is developed. The background, theory and experimental results that demonstrate the feasibility of such a system are presented and the results are compared with the performance of existing fiber-based means of measuring temperature. Experiments on several OTDR-addressed, intensity-based optical temperature sensors are performed and a method for manufacturing small air gap splices for use in measuring strain at several places along an optical fiber are presented.

ACKNOWLEDGEMENTS

This thesis is dedicated in loving memory to my late mother, Anna Marie Jacobson, who passed away December 4, 1988. Active in education for years, her last request to me was that I finish my studies at Virginia Tech even though she knew she would not be here to watch me graduate.

I wish to thank my advisor and committee chairman, Dr. Richard O. Claus for his help and encouragement. I would also like to thank Dr. Ira Jacobs and Dr. Ting-Chung Poon for serving on my committee.

I would like to thank Mr. James H. Davis of the Naval Sea Systems Command for getting me started in fiber optics and encouraging me along the way.

I am grateful to all the students and staff members at the Fiber and Electro-Optics Research Center for their help during my stay here at Virginia Tech. I am especially indebted to Brad Duncan, Joe Ingold, Cloyd Tavenner, Sara Moneyhun, Daniel Thomas, Melanie Ott, Hamid Abedi, and Shari Feth, who helped me in my classes. I am also grateful to Bernd Zimmermann, Kent Murphy, Mike Gunther, Jeff Andrews, and Mark Miller, who helped me with my research and thesis.

I would also like to thank my father, Peyton Jacobson, and my sister Ellen Wilson and her family as well as my good friends Mr. Ray "Rock" Hudson and his wife Jean for their encouragement and support.

Finally, I would like to express my extreme gratitude to the many close friends I made here in Blacksburg. Too numerous to mention them all, I am especially grateful to Carl York, Kevin Trainum, Samantha Sinclair, Jonathan Hodge, Robin Roylance, Harry Telegadas, John Salm, Ed Moas, Tom Baxter, and Wallyball Team Captain Joe "The Shark" Meyers for sharing their experience, strength and hope.

Thank you all for helping me through this ordeal known as "college after age thirty-five".

TABLE OF CONTENTS

ABSTRACT..... ii

ACKNOWLEDGEMENTS..... iii

LIST OF FIGURES..... vi

1.0 INTRODUCTION..... 1

2.0 OTDR..... 3
2.1 THE BASIC OTDR SYSTEM..... 3
2.2 THE PHOTON COUNTING OTDR..... 4

3.0. STRAIN MEASUREMENTS USING OTDR..... 8
3.1 STRAIN..... 8
3.2 MEASURING STRAIN..... 9
3.3 ESTABLISHING REFERENCE MARKS..... 11
3.4 THERMAL CONSIDERATIONS..... 13

4.0 EVOLUTION OF THE OVERALL STRAIN SENSOR DESIGN..... 20
4.1 INTENSITY MODULATION..... 21
4.11 THE MOVING MASK..... 22
4.12 FIBER DISPLACEMENT..... 22
4.13 WAVEGUIDE COUPLING..... 23
4.14 MICROBEND LOSS..... 23
4.2 THE INTENSITY MODULATED TEMPERATURE SENSOR PORTION--DETAILED DESIGN..... 24
4.3 SENSOR CONSTRUCTION..... 26

5.0 EXPERIMENTATION..... 34
5.1 STRAIN TESTING--TEMPERATURE CONSTANT..... 34
5.2 TEMPERATURE EFFECTS..... 34
5.3 THE LOW-RANGE TEMPERATURE SENSOR..... 35
5.4 THE MEDIUM RANGE TEMPERATURE SENSOR..... 36
5.5 THE HIGH RANGE TEMPERATURE SENSOR..... 37
5.6 SENSOR REDESIGN..... 37

6.0 DISCUSSION OF RESULTS..... 44

7.0 CONCLUSIONS AND RECOMMENDATIONS..... 46

REFERENCES..... 48

VITA..... 50

LIST OF FIGURES

FIGURE

2.1 The Basic ODTR..... 6

2.2 An OTDR plot..... 7

3.1 Linear Strain..... 16

3.2 The Neck-Down Aberration..... 17

3.3 The Double-Sphere Aberration..... 18

3.4 Temperature Compensated Strain Sensor Design,..... 19
Phase I

4.1 Temperature Compensated Strain Sensor Design,..... 28
Phase II

4.2 Temperature Compensated Strain Sensor Design,..... 29
Phase III--Final

4.3 Intensity Modulated Temperature Sensors..... 30

4.4 Graph of Air Gap vs Intensity..... 31

4.5 Air Gap vs Intensity--Theoretical Plot..... 32

4.6 Temperature Sensor Detail Design..... 33

5.1 Strain Sensor Test Setup..... 39

5.2 Temperature Sensor Test Setup..... 40

5.3 Results of the Low Range 41
Temperature Sensor Test

5.4 Results of the Medium Range 42
Temperature Sensor Test

5.5 Results of the Redesigned Low Range..... 43
Sensor Test

CHAPTER I

1.0 INTRODUCTION

Strain measurement using optical fiber is a relatively new technology with several methods having been developed over the past few years. The Interferometer [1,2] which has been developed and refined by the Naval Research Laboratory, the Intensity Modulator [3], the Modal Domain sensor proposed by Duncan [4], and Zimmermann's method using Optical Time Domain Reflectometry (OTDR) [5] are examples of fiber optic sensors that can be used to measure strain. Others who have investigated the use of OTDR for sensing are Jackson et. al. [6], Kingsley [7,8], Sirkis [9], and Kim et. al. [10].

One problem with fiber optic strain sensors is the effect of temperature on the strain measurement. As will be discussed later, both refractive index and fiber geometry vary with temperature and these variations can affect strain measurements.

A fiber optic strain sensor that would compensate for temperature effects was desired. The method chosen was to expand on Zimmermann's technique [5] which uses OTDR to measure strain between air gap splices. The air gap splices

cause pulses on the OTDR and these pulses shift as the fiber between them is strained. One area to be expanded upon was the manufacturing of the air gap splices. The desired result was to make them easy to manufacture and as small as possible so they could be embedded in a material and subsequently used for internal material measurements.

The purpose of this thesis, then, is twofold: 1) To develop a means of temperature compensation for strain measurements taken with an OTDR and 2) To develop small, easy-to-manufacture substitutes for large cross-section air gap splices previously used in OTDR Fresnel-based strain measurements.

The method proposed here for measuring temperature compensated strain is believed to be novel. To our knowledge no one has combined an intensity temperature sensor and an OTDR strain measurement technique as reported here to obtain temperature compensated strain measurements.

CHAPTER II

2.0 OTDR

An optical engineer uses OTDR to measure the overall loss in optical fiber and to locate breaks, microbends or other aberrations.

In an OTDR-based fiber optic strain sensor, an OTDR is used to observe the relative movement of two marked points as the fiber is strained [5]. Since the marked points (simply aberrations in the fiber) may be relatively close together and may move only a small distance, an OTDR with high resolution is needed to measure small strains in small structures. The OTDR used in the experiments reported here was the Opto-Electronics Picosecond Fiber Optic System which consists of the MF-20 Mainframe and the TDR10 Processing System and is rated at 100 micron resolution [11].

2.1 BASIC OTDR SYSTEM

The typical basic OTDR system consists of a pulsed laser, a detector, averaging circuitry and an output screen on an oscilloscope. A block diagram of this basic OTDR is shown in Figure 2.1 [12]. The pulsed laser light is coupled into the

fiber and the backscatter is sent back to a beamsplitter or fiber coupler and is partially received by the photodetector. The averager and additional signal processing electronic circuitry is used to improve the signal to noise ratio and display the backscatter.

The resultant plot on the oscilloscope generally is a negatively sloped function from which the Rayleigh backscatter may be inferred. Localized large amplitude pulses in the output represent Fresnel reflections. A simple OTDR plot is shown in Figure 2.2 [12]. For this work, however, only the Fresnel reflections were monitored.

It should be noted that Rayleigh backscatter can be used to measure strain, but it is complicated by the spatial transient behavior of the fiber. A localized strain causes some backscatter above that caused by normal Rayleigh effects and thus limits the spatial resolution. This effect can be minimized by segmenting the fiber [5].

2.2 PHOTON COUNTING OTDR

A more sensitive OTDR is the photon counting OTDR. Here the OTDR counts photons to determine the amount of light at the photodetector. Typically the photon counting OTDR uses

an avalanche photodiode in the "geiger counter" mode. A minimum detector sensitivity of 16 photons has been reported [13], and experiments with single photon avalanche diodes (SPAD) have resulted in a minimum sensitivity of 3×10^{-15} watts [14]. Opto-Electronics reportedly is in the process of manufacturing a photon counting detector for use with the OTDR at the Fiber and Electro Optics Research Center at Virginia Tech. As will be discussed later, the use of this detector would allow new methods of OTDR strain measurement to be undertaken.

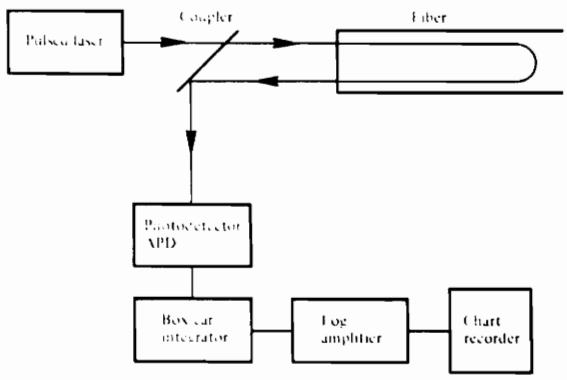

Figure 2.1 The Basic ODTR

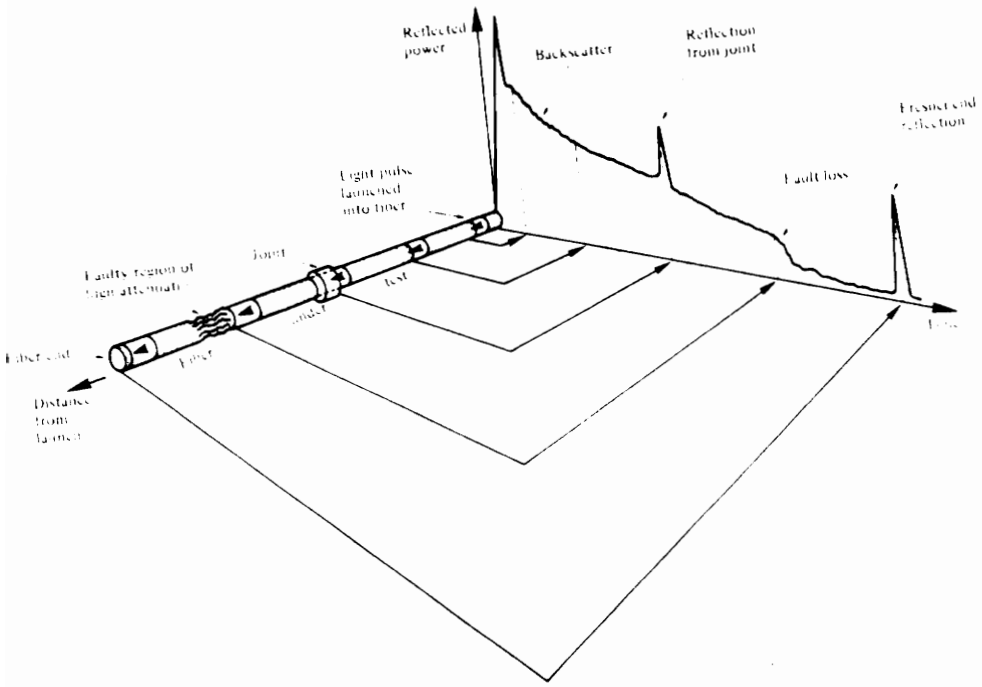

Figure 2.2 An OTDR plot

CHAPTER III

3.0 STRAIN MEASUREMENTS USING OTDR

3.1 STRAIN

For the purposes of this project, the discussion of strain will be limited to linear, or "one-dimensional" strain since that is what happens when an optical fiber is strained.

Figure 3.1 shows an object being strained by a force "F". When the force is applied, points A and B move to the positions A' and B' respectively. The displacement of point A is u and the displacement of point B is $u + \Delta u$. The definition of linear strain ϵ is therefore

$$\epsilon = \lim \Delta u/\Delta x = du/dx \qquad (3.1)$$

It should be noted that Figure 3.1 ignores the Poisson effect, which is the tendency of an object under tensile strain to contract laterally [15].

3.2 MEASURING STRAIN

As shown in chapter II, Fresnel reflections occur at the location of a material interface along the fiber. When using OTDR techniques to measure strain, one purposely places two or more sets of interfaces along the fiber and measures the amount of separation between the resultant OTDR pulses in the time domain. The time separating the pulses will increase as the fiber is strained because the length of the fiber increases. Note, however, that the pulses may also be characterized by their amplitude as well as their location in time. In this thesis, modulation of pulse amplitude is used to determine temperature. Measurement of pulse spacings and amplitudes results in two readings: temperature (related to pulse amplitude) and strain-plus-temperature (related to pulse separation change). It is theorized that the temperature effects can be subtracted from the strain-plus-temperature effects to give us a measurement of strain only.

Zimmermann presented the basic theory for determining strain at constant temperature [5]. It is presented here briefly.

The length of the fiber, l_f, is given by

$$l_f = ct/n \tag{3.2}$$

where c is the speed of light, t is the time it takes the light pulse to travel the length of the fiber and n is the group index of refraction of the fiber core. Differentiating equation 3.2 gives an expression for the amount of fiber elongation.

$$dl_f = (c/n^2)(ndt - tdn) \tag{3.3}$$

The strain, ϵ, is given by

$$\epsilon = dl_f/l_f$$

$$= dt/t - dn/n. \tag{3.4}$$

The relationship between index and strain is assumed linear and the proportionality constant is defined as "a", a negative number that can be determined empirically. In his experiments, Zimmermann found "a" to range between -0.27 to -0.36 depending on the fiber type

Assume dn/n is given by

$$dn/n = a(\epsilon) \tag{3.5}$$

The equation for strain, equation 3.4, is now

$$\epsilon = (dt/t)(1/(1 + a)) \qquad (3.6)$$

where dt is the shift in pulse arrival time between the unstrained and strained states.

3.3 ESTABLISHING REFERENCE MARKS

Establishing small, easy-to-manufacture OTDR addressable reference marks along a fiber was another purpose of this effort. The two methods as shown in Figures 3.1 and 3.2 were attempted. The first of these was the fiber "neck-down" approach. With a fiber connected to the OTDR, a portion of 100/140 multimode "semi-graded" (effective index profile >2) index fiber was placed in the fusion splicer (Power Technology, Inc., Model PFS 330). An arc was then generated while providing a tensile force on the fiber. This resulted in a slight necking down of the fiber. The process was then repeated, in an attempt to get an OTDR pulse reflected from the location of the neck-down area, while maintaining the end reflection.

It was determined that by the time the fiber had necked

down enough to produce a back reflection, there was not sufficient power transmitted to observe the far end reflection.

Another attempt at establishing a reference mark was to create rounded ends on two fibers prior to fusing. While the ends were still separate, they were brought together on the fusion splicer guides until a Fresnel reflection was detected. The spheres were then fused, attempting to keep them separated at the distance that gave the highest Fresnel reflection.

This method was attractive because the reference mark was fast and easy to manufacture compared to an encapsulated tube air gap splice. While the spheres gave a Fresnel reflection, the resultant decrease in power transmitted through the mark was too great to give a second reflection.

While neither of these attempts were successful using the Opto-Electronics OTDR, they may work when used with a Rayleigh backscatter/photon counting OTDR. The potential increased sensitivity obtainable using such devices would warrant an investigation of these designs.

3.4 THERMAL CONSIDERATIONS

As Zimmermann pointed out, the effects of temperature on the sensor output are due to changes in both refractive index and in fiber length [5]. The refractive index changes, however, are the dominant effects. The combined effect of temperature on time delay is:

$$\partial\tau/\partial T = (1/c)((\partial n/\partial T)l_f + n(\partial l_f/\partial T)), \quad (3.7)$$

where

$$\partial l_f/\partial T = \alpha l_f, \quad (3.8)$$

and α is the Coefficient of Thermal Expansion of the fiber. Typical values are 7×10^{-7} m/m-°C for α and 2×10^{-5}/°C for $\partial n/\partial T$ [5]. Substituting these values into equations 3.7 and 3.8, we would expect to see a change in time delay of 20 ps for a one-way measurement or 40 ps for a two-way measurement for a 3-meter length of fiber and a 100°C temperature rise.

It was theorized that if a measurement of temperature was obtained where the strain was being measured, equations 3.6, 3.7 and 3.8 could be used to determine the strain independent of temperature effects. The following is a sample calculation:

Assume 3 meters of fiber is strained 2%. Typical values are:

$$\Delta\tau = 20 \text{ ps}$$

$$\tau = 1450 \text{ ps for } n = 1.45$$

$$a = -.3$$

$$\epsilon = (\Delta\tau/t)(1/(1+a)) \tag{3.6}$$

$$= (20/1450)(1/.7) = .02 = 2\% \text{ strain}$$

In other words, if this fiber is strained under constant temperature, and a pulse shift of 20 picoseconds is observed, a strain of 2% has taken place.

If the temperature increases 50°C, the pulse shift due to temperature alone is given by

$$\partial\tau = (1/c)((\partial n/\partial T)l_f + n(\partial l_f/\partial T))\partial T. \tag{3.7}$$

Typical values are:

$$\partial n/\partial T = 2 \times 10^{-5}/^{\circ}C$$

$$\partial l_f / \partial T = \alpha l_f \qquad (3.8)$$

$$= .21 \times 10^{-5} \text{m/m-°C for 3 meters}$$

$$\Delta\tau = (1/(3\times10^8))(6 \times 10^5 + (1.45)(.21)(10^{-5})(50)$$

$$= 10.5 \text{ ps}$$

$$\epsilon_{apparent} = (20-10.5)/(1450)(1/.7) = .009 = .9\% \text{ strain}$$

$$\text{error} = (2 - .9)/2 = 55\%$$

Thus in a typical case an error of 55 percent could be corrected if accurate temperature measurement were obtained.

The overall design shown in Figure 3.3 was proposed for the temperature compensated strain sensor. The figure shows the fiber with reference marks for the OTDR-based sensor reflections. Between the strain measuring fiber and the OTDR, an intensity modulator that is temperature sensitive is inserted. The amplitude of the OTDR pulses will fluctuate as a function of temperature.

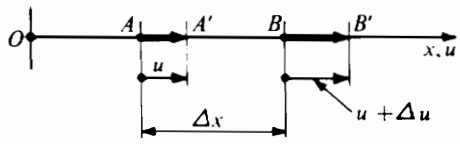

Figure 3.1 Linear Strain

Figure 3.2 The Neck-Down Aberration

Figure 3.3 The Double-Sphere Aberration

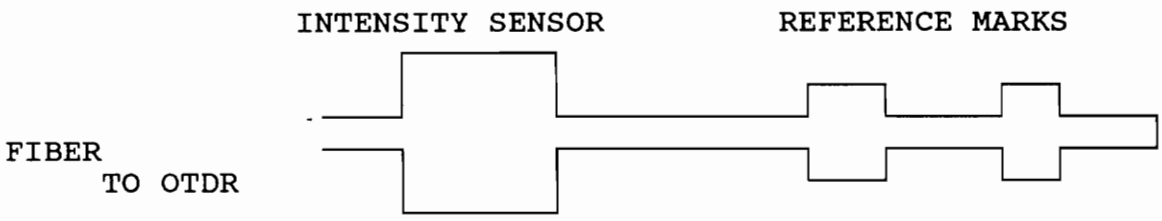

Figure 3.4 Temperature Compensated Strain Sensor Design, Phase I

CHAPTER IV

4.0 EVOLUTION OF THE OVERALL STRAIN SENSOR DESIGN

As mentioned in chapter III, initial attempts at creating the novel, in-line reference marks along the sensor fiber were not successful. The plan was to use the design shown in Figure 3.3 for the temperature compensated strain sensor and to make the air gap splices as easy as possible to manufacture. Since neither the double-sphere nor the neck-down design worked (though either of these may work with a photon counting OTDR), it was felt that the best design would be to use air gap splices similar to those Zimmermann used in his experiments. One possible problem with this, though, was that the air gap splices themselves might expand with temperature (though this could be prevented by encapsulating the splices) and would therefore reduce the pulse amplitude by increasing the distance of the gap across which the light must travel. Also, it was desired to make the sensor as straightforward and simple as possible.

The overall strain sensor design was reconsidered and it was noticed that one air gap splice could be eliminated and the far end reflection would be used for the second reference mark. This would then give us two pulses on the OTDR. The

design is shown in Figure 4.1.

The design was reevaluated further. Still present was the remaining air gap splice. It was determined that this splice could be eliminated entirely and only the pulses resulting from the intensity temperature sensor and the far end reflection would be used. This would simplify the manufacturing of the sensor. As can be seen in Figure 4.2, the final design of the temperature compensated strain sensor consists of a temperature sensor with a length of fiber connected to it. When the length of fiber is strained, the two pulses on the OTDR will separate. The pulse caused by the mark closest to the OTDR will remain stationary and the other one will move.

Having reviewed the macroscopic design of the strain sensor, an examination of the design of the intensity temperature sensor follows.

4.1 INTENSITY MODULATION

A result of optical intensity modulation is that the amplitude of a pulse seen on the OTDR output display will vary with temperature. Four basic types of intensity modulation were considered: Moving mask, fiber end displacement,

waveguide coupling, and microbend loss. These are described below [16].

4.11 MOVING MASK

As can be seen in Figure 4.3(a), the "moving mask" device consists of two fibers, each connected to a lens and a blocking device or mask. The mask may move between the two lenses and block out part of the transmitted light. If the mask is attached to a bimetallic strip in a mechanical housing, the mask will move in and out as a function of temperature.

Note that this method can be used with or without the lenses. The only difference between the two cases is that when no lenses are used, the sensitivity is reduced by the loss over the gap between the fibers.

4.12 FIBER DISPLACEMENT

Fiber displacement is a rather simple method of modulating transmitted light intensity. See Figure 4.3(b). Here the fiber moves either laterally or longitudinally as a function of temperature. The amount of light coupled into the receiving fiber will therefore be a function of temperature.

4.13 WAVEGUIDE COUPLING

With this method the cladding from two sections of fiber is removed so the evanescent fields are coupled from one fiber into the other. See Figure 4.3(c). If metal, or other material that expands as a function of temperature, is attached to the two fibers, then as the fibers move away from each other, the light intensity coupled into the receiving fiber is reduced.

4.14 MICROBEND LOSS

Another sensor is the microbend sensor shown in Figure 4.3(d). Here the fiber is configured in small bends and a deformer is used to squeeze the fiber and thus decrease the bend radii. As the fiber bends are made smaller, some of the light then propagates into the cladding which gives a loss in intensity.

4.2 THE INTENSITY MODULATED TEMPERATURE SENSOR PORTION, DETAILED DESIGN

As described above, there are several ways to design an intensity-based temperature sensor. For this project, the sensor design chosen was one that had a longitudinal air gap that increased with temperature. The main reason for choosing this sensor was ease of manufacturing.

The first task in designing the sensor was to determine the distance the air gap would have to increase to give optimum sensitivity. This was done by placing the two cleaved ends of 100/140 fiber into the fusion splicer and then varying the air gap. The gap was varied in increments of 50 microns while the intensity of the far end reflection was observed. The air gap gave a noticeable intensity drop at 50 microns and still transmitted a readable signal with a gap of 600 microns. The data is shown in the graph in Figure 4.4.

It was desired to compare this plot with the theoretical loss of the fiber over a transverse air gap. Several articles [17-21] have been written on the subject and the method of calculating the loss using ray optics is given by Miller and Mettler [17].

Figure 4.5 gives a plot of the theoretical power reduction over the air gap. Note that this curve matches quite well with the actual data taken. The slight differences can be attributed to mode mixing [18].

The next task was to design the temperature sensor and select the material. The temperatures ranges chosen were 23-100°C, 23-180°C, and 23-350°C full scale. The tubing material selected was corrosion resisting steel (CRES) because of its relatively high coefficient of thermal expansion, 17.3 x 10^{-6}cm/cm-°C [22].

Another problem was how to attach the fiber to the casing. For this TRA-CON epoxy was chosen because in other experiments it proved easy to use and had exhibited good adhesion characteristics.

One important aspect of the manufacturing of the intensity sensor device is obtaining clean perpendicular faces on the fiber ends that form the air gap. Better reflections and light transmission through the temperature sensor are possible when proper cleaving is employed. To obtain good cleaves the York FK-1000 cleaver was used.

4.3 SENSOR CONSTRUCTION

The sensors were 2.5 cm, 7 cm, and 15.25 cm long. Each consisted of a stainless steel tube surrounding a hollow core fiber which was epoxied at one end to the tube and the fiber. At the other end the tube was epoxied to the 100/140 fiber end and the hollow core fiber was allowed to float free. See Figure 4.6.

The 2.5 cm long sensor was to be the high temperature sensor, designed to operate from room temperature (23°C) to 350°C, a ΔT of approximately 320°C. The 7 cm sensor was designed to operate from room temperature to 180°C, a ΔT of about 160°C. The 15.25 cm long sensor was the low temperature sensor, designed to operate over a temperature range of approximately 80°C, from room temperature to 100°C.

The 7 cm sensor was built using "active manufacturing"; that is the two fiber ends that form the air gap were placed into the hollow core fiber while one end of the 100/140 fiber was connected to the OTDR. This way it could be determined whether or not adequate reflections were present on the OTDR as the sensor was built. The last step was to epoxy the sensor at the ends of the metal tube. This was also done actively to ensure pulses due to the two reflections were on

the OTDR screen when the unit was left to allow for epoxy curing.

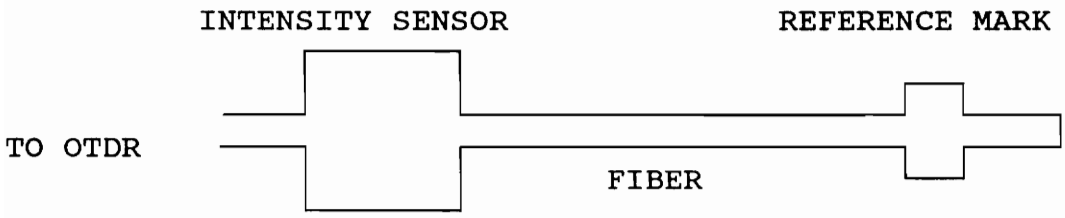

Figure 4.1 Temperature Compensated Strain Sensor Design, Phase II

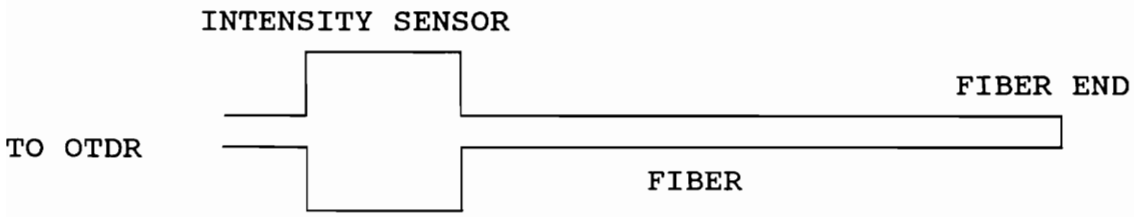

Figure 4.2 Temperature Compensated Strain Sensor Design, Phase III--Final

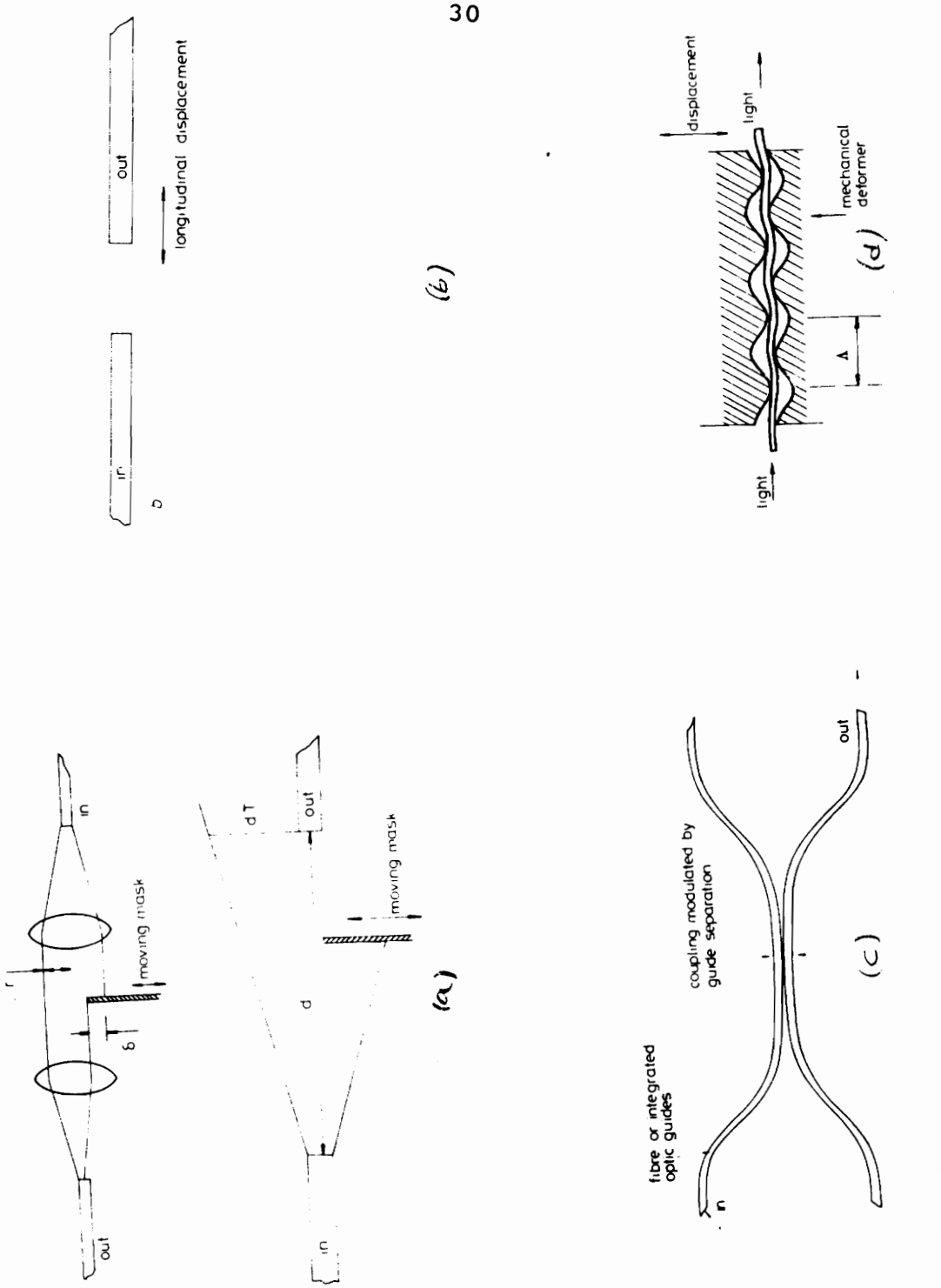

Figure 4.3 Intensity Modulated Temperature Sensors

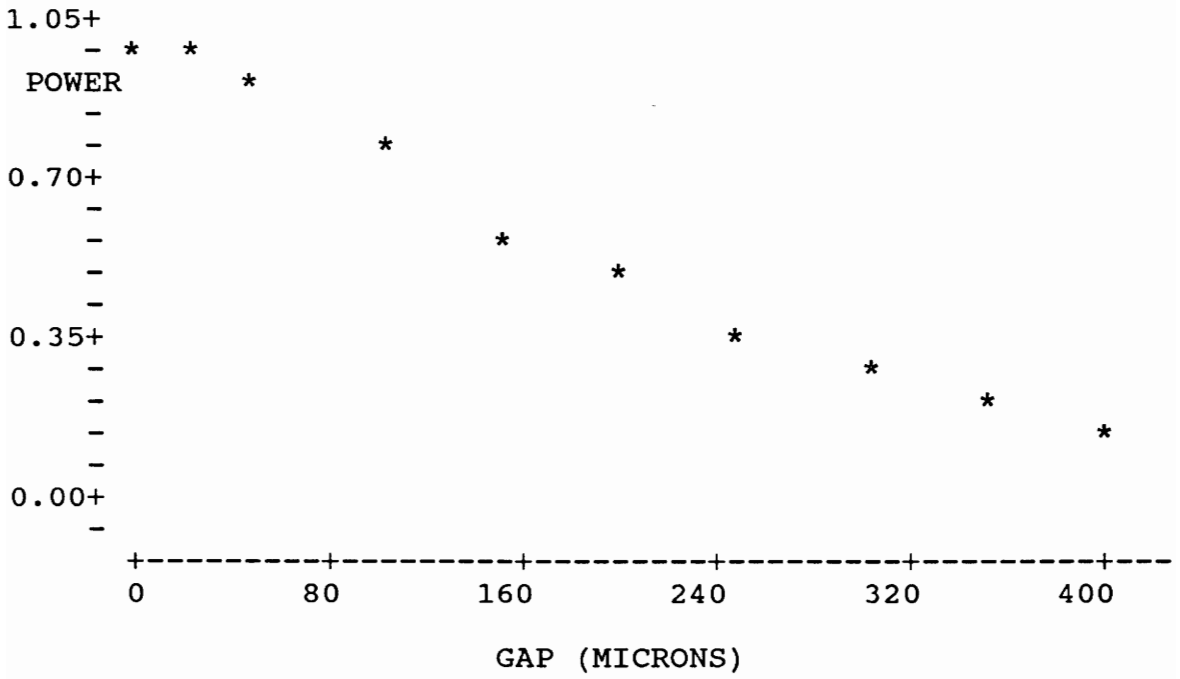

Figure 4.4 Graph of Air Gap vs Intensity

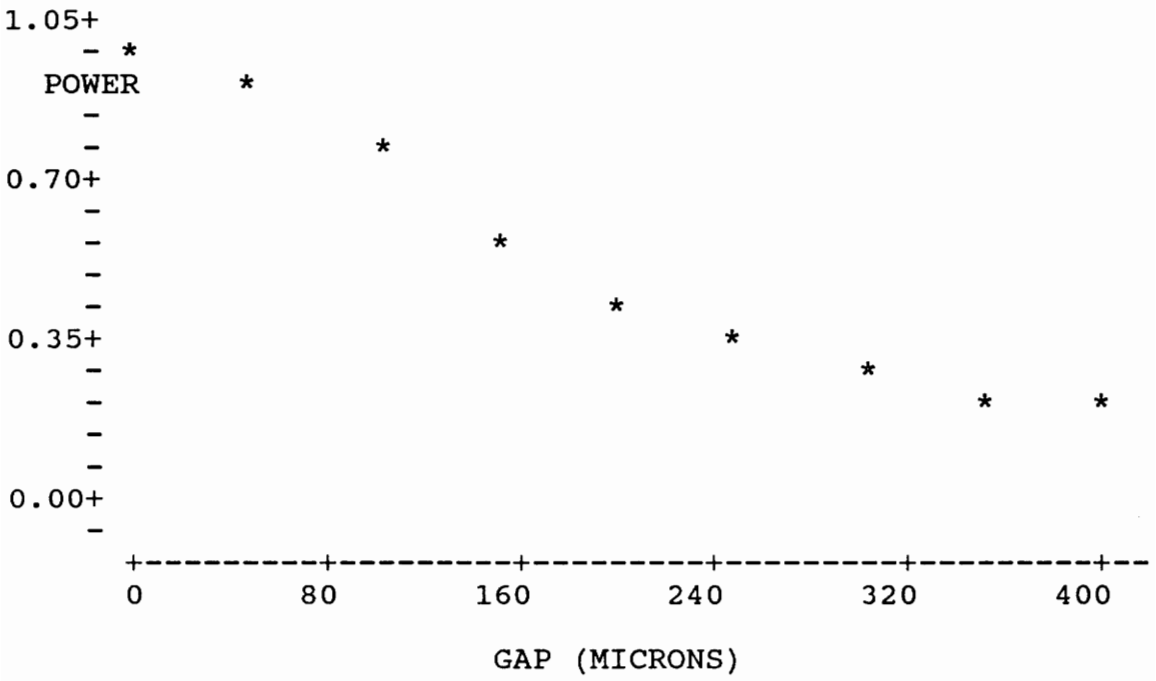

Figure 4.5 Air Gap vs Intensity--Theoretical Plot of Power Loss Over an Air Gap

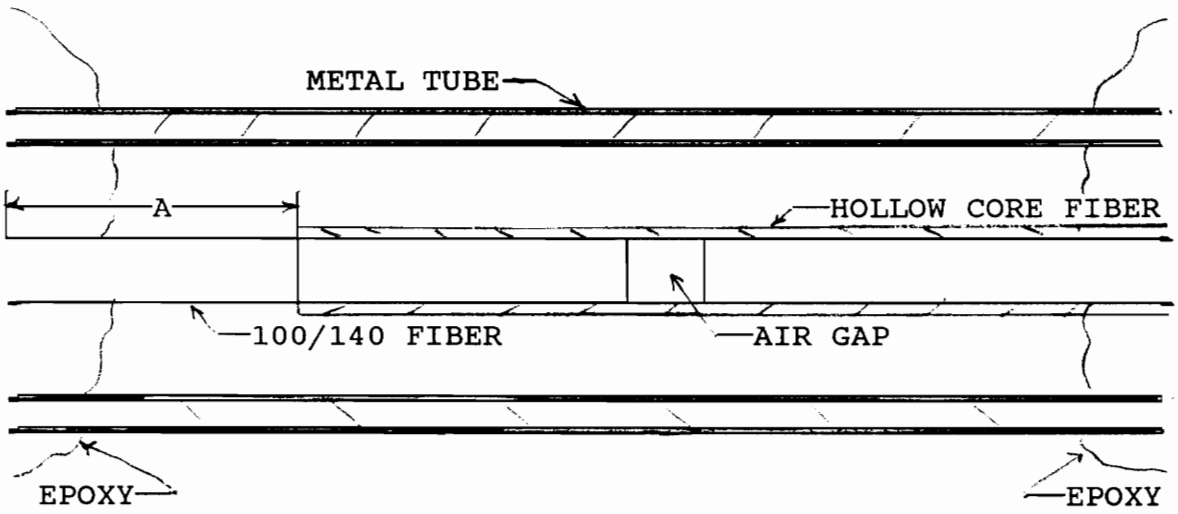

Figure 4.6 Temperature Sensor Detail Design

CHAPTER V

5.0 EXPERIMENTATION

5.1 STRAIN TESTING--TEMPERATURE CONSTANT

An experiment to test the strain measuring capabilities at constant temperature was set up as shown in Figure 5.1. The pulley was loaded, thus straining the fiber and the result was a pulse shift. This experiment confirmed that strain between two points could be measured with the temperature constant.

5.2 TEMPERATURE EFFECTS

In order to determine the pulse shift due to temperature only, a 3-meter length of fiber was placed in the Thermotron at room temperature and the setup was prepared for a 100°C temperature rise while the far end pulse was monitored on the oscilloscope. The expected pulse shift had been calculated to be approximately 40 ps.

The pulse was monitored under room temperature conditions. A shift as much as 44 ps due to the instability of the OTDR system was noticed. The system had been unstable

in earlier experiments by other FEORC students and long-term stability was necessary for this experiment. The conclusion was that accurately measuring the pulse shift due to temperature only would not be possible until OTDR problems were resolved.

In order to evaluate the temperature sensors, testing devices and procedures were developed. In two cases, the OTDR was connected to the sensor and the sensor was placed in a water bath as shown in Figure 5.2. The other times the sensors were tested in the Thermotron oven and the amplitude of the pulses at the far end reflections were observed. Note that the devices were not strained.

5.3 THE LOW-RANGE TEMPERATURE SENSOR

The low-range temperature sensor was tested by placing it in a beaker of water on a hot plate. As the temperature increased, no change was found in the amplitude of the far end reflection. Also, the amplitude of both the sensor gap peak and the far end reflection were extremely small. This led to the belief that some damage had occurred to the ends of the fiber forming the air gap. It most likely had broken when the fiber was inserted into the hollow core.

Another low-range sensor was manufactured with the same dimensions. This time the sensor was constructed while it was connected to the OTDR. This way it was possible to monitor the reflections while the fiber was being inserted into the hollow core. Since a good reflection was maintained throughout the manufacturing process, it appeared the cleaved fiber faces were still flat and smooth. This proved to be the case. This sensor was tested in the Thermotron oven and the results are shown in Figure 5.3.

5.4 THE MEDIUM-RANGE TEMPERATURE SENSOR

The 7 cm sensor was tested by placing it in a beaker of water and then putting the beaker on a hot plate. The sensor was connected to the OTDR and the hot plate was turned on. Temperature readings were taken at approximately every 10°C. The results are shown in the graph, Figure 5.4.

As the temperature neared the boiling point of water, (actually 97°C), the sensor was placed directly on the hot plate to see what would happen. The intensity of the pulse dropped rapidly. Since no means of measuring the temperature directly on the hot plate was available, no data was recorded. This experiment lead to the belief that the sensor was actually more effective at a higher range than 20 to 100°C.

Most likely too much epoxy had wicked into one of the ends of the stainless steel tube, thus decreasing the effective length of the tube.

5.5 THE HIGH-RANGE TEMPERATURE SENSOR

Since the range of the 2.5 cm long, high-range temperature sensor was relatively high, it was placed directly on the hot plate and the signal amplitude was observed. The signal decreased in amplitude as the temperature increased. Unfortunately, during manufacture, the fiber jacket had been stripped away from the metal tube a distance of about 10 cm. This made the fiber weak in that area and it broke as the sensor was placed in a beaker of water to cool it down and watch the signal increase in amplitude.

We did not repeat the above experiments because the first trial showed that the sensors were not satisfactory.

5.6 SENSOR REDESIGN

Brass was the material chosen for the redesigned sensor. The sensor was 15.25 cm long and an initial air gap was intentionally inserted between the fibers at room temperature. This sensor was manufactured actively. The initial gap size

was increased until the signal strength of the far end reflection dropped one division on the oscilloscope. The sensor was tested in the Thermotron oven for two full temperature cycles from 23°C to 120°C. The results are shown in Figure 5.5.

Notice that the plot is fairly linear and has good low end sensitivity. Note also that the sensor gives good signal variation over the temperature range. This is due to the higher coefficient of thermal expansion of brass vs. CRES.

The results, however, were not repeatable. A likely explanation of this is the magnitude of the distance A shown in Figure 4.6. When the sensor was manufactured, it was desired to keep A fairly large so the epoxy did not wick into the tube to the free end of the hollow core fiber. This would stop the relative movement between the fiber and the hollow core and thus make the sensor ineffective.

The results show, however, that A had been made too large. The fiber had most likely bowed when the outer tube had shortened due to cooling. This bowing would have caused the hysteresis.

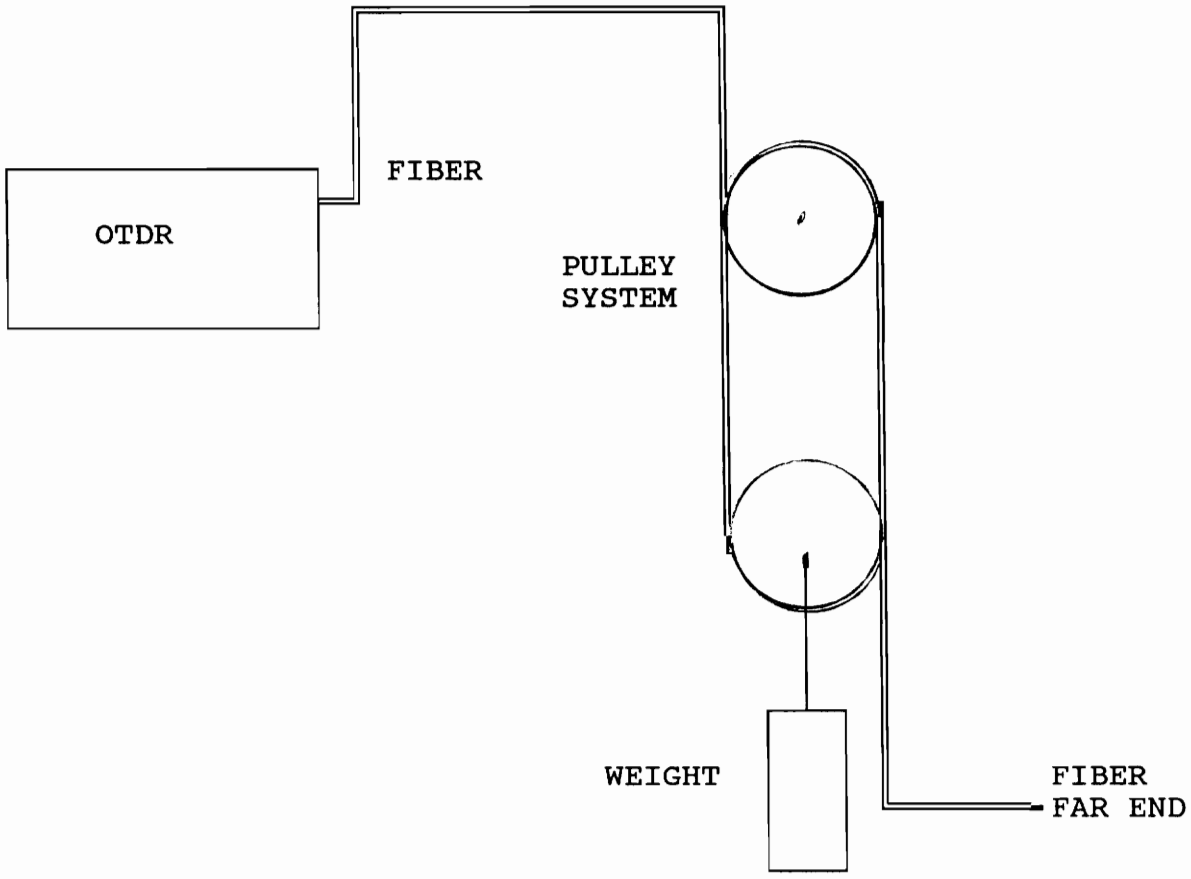

Figure 5.1 Strain Sensor Test Setup

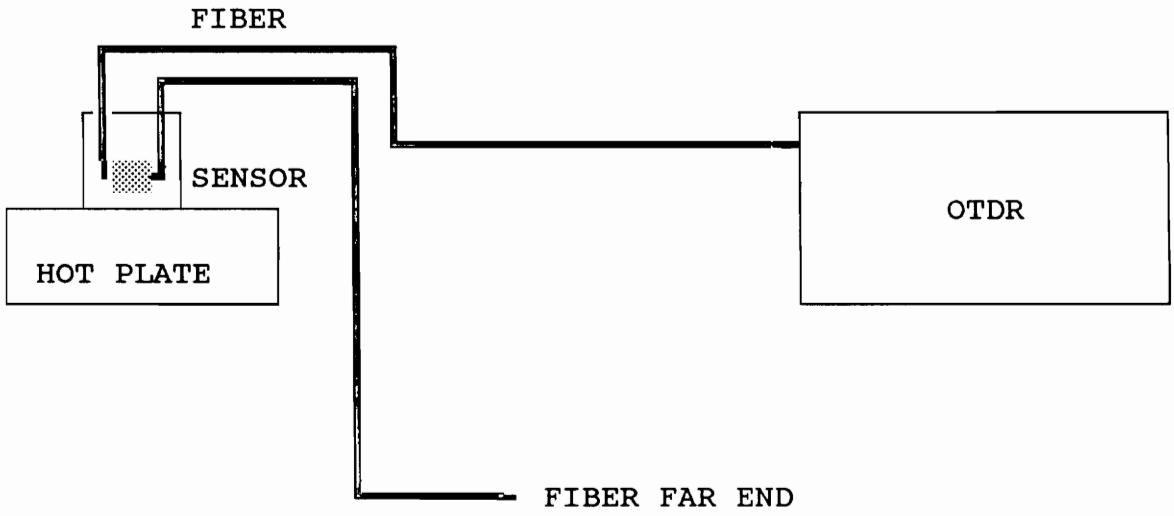

Figure 5.2 Temperature Sensor Test Setup

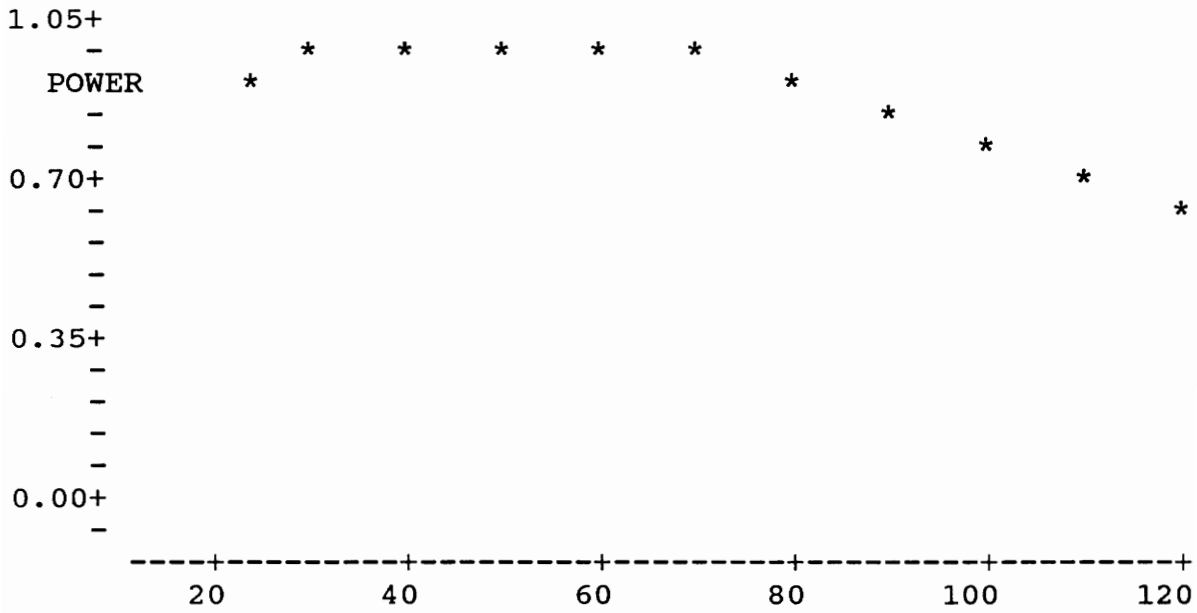

Figure 5.3 Results of the Low Range CRES Sensor Test

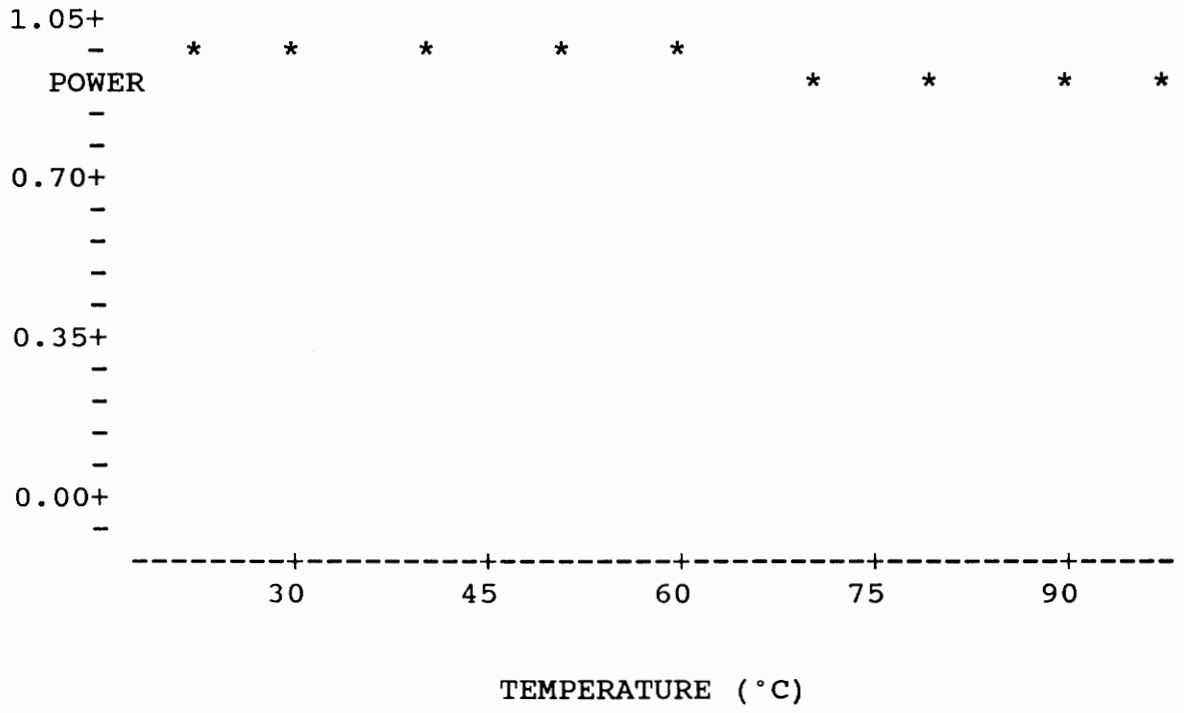

Figure 5.4 Results of the Medium Range Brass Temperature Sensor Test

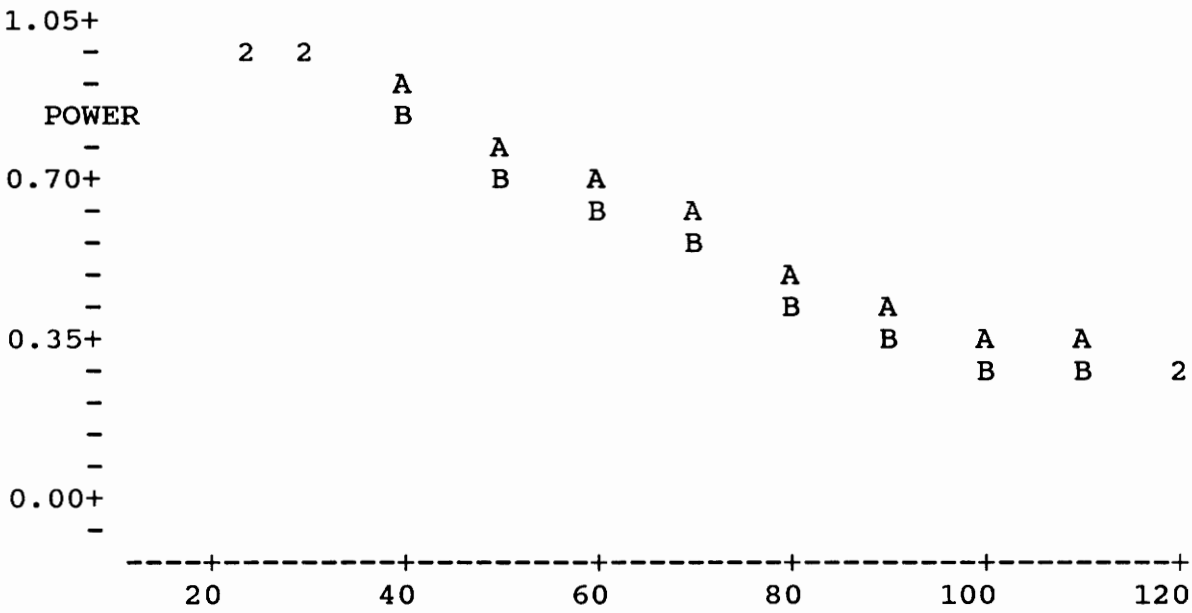

A = SIGNAL VS TEMPERATURE--FIRST TRIAL

B = SIGNAL VS TEMPERATURE--SECOND TRIAL

Figure 5.5 Results of the Redesigned Sensor Test

CHAPTER VI

6.0 DISCUSSION OF RESULTS

The results shown in Figures 5.3, 5.4, and 5.5 show that problems existed with all sensors and that the redesigned brass sensor was the best of the three.

The difference between the two stainless steel sensors can be attributed to the initial gap (or lack thereof) between the two cleaved fibers. In the low range temperature sensor there was no initial gap inserted when the sensor was constructed. An explanation of the peak between 30°C and 70°C is that there exists a certain amount of total internal reflection between the two cleaved fiber ends and the inside of the hollow core fiber when the gap is very small. This internal reflection could be setting up a Fabry Perot effect that gives the peak.

With the medium range stainless steel sensor, the curve is relatively flat with a slight decrease at 70°C. Since this sensor was shorter than the low range temperature sensor (7 cm vs 15.25 cm), it was expected the curve would be somewhat flat, but not to the degree that was observed. This sensor may have had an increase in the size of the initial gap while

the sensor was being cured. This would have made the sensor give a smaller decrease in power for a given temperature range. Figures 4.4 and 4.5 show that the power loss curve flattens out after the gap size exceeds 250 microns.

Both of these stainless steel sensors had curves that were unsatisfactory. However, ignoring the low end peak, the low range sensor had a 40% power reduction over a 50°C temperature range.

With the redesigned sensor, equivalent in length to the low range stainless steel sensor, brass was chosen because it had a 21% higher CTE over stainless steel [22]. The brass sensor had a 50% reduction in power over a 50°C range. This is what would be expected because of the higher CTE.

The main problem with the brass sensor was the repeatability. It appears that the A dimension shown in Figure 4.6 was too large, thus causing a bowing effect on the fiber. Also, since the diameter of the metal tube is much larger than the fiber, some misalignment no doubt occurred.

CHAPTER VII

7.0 CONCLUSIONS AND RECOMMENDATIONS

A method of compensating for temperature when making strain measurements using Fresnel-based Optical Time Domain Reflectometry has been presented. The method relies on a temperature sensitive in-line element that modulates the intensity of light received from a far fiber end reflection. In developing this strain sensor, several intensity temperature sensors were designed and constructed. These sensors have various operating temperature ranges and were made using both corrosion resistant steel and brass. Brass elements produced better temperature effect reduction of the pulse amplitude.

Both the overall strain sensor and the temperature sensor designs are described. The initial strain sensor design was simplified and the performance of the temperature sensor was improved. Although the problem of hysteresis existed, a solution was presented, namely decreasing the length of free fiber inside the tube. However, misalignment of the fibers inside the tube could be present.

A recommendation is that the two reference mark methods

developed herein be tested with a photon counting OTDR. Due to the repeatability problems and the extreme difficulty in manufacturing and aligning the sensor components, this design cannot be recommended as a temperature corrected strain measuring device. The concept of using two sensing techniques could perhaps be put to better use with more sophisticated sensor designs.

REFERENCES

1. T.G. Giallorenzi, J.A. Bucaro, A.D. Dandridge, G.H. Siegel, J.H. Cole, S.C. Rashleigh, and R.C. Priest, "Optical Fiber Sensing Technology," IEEE J. Quantum Electronics, QE-18, pp 626-665.

2. J.S. Sirkis and C.E. Taylor, " Interferometric-Fiber-Optic Strain Sensor," Experimental Mechanics, June 1988, pp 170-176.

3. B. Culshaw, Optical Fibre Sensing and Signal Processing, copyright 1984, Peter Peregrinus Ltd., London pp 64.

4. Brad Duncan, "Modal Domain Sensing," Master's Thesis, Virginia Polytechnic Institute and State University Department of Electrical Engineering, January, 1988.

5. B.D. Zimmermann, "High Resolution Optical Time Domain Reflectometry and its Applications," Master's Thesis, Virginia Polytechnic Institute and State University Department of Electrical Engineering, January, 1988.

6. R.O. Claus, B.S. Jackson, and K.D. Bennett, "Nondestructive Testing of Composite Materials by OTDR," SPIE Conference Proceedings, June 23-28, 1985, pp 243-247.

7. S.A. Kingsley, "Advances in FODAR (Fiber Optic Detection and Ranging)," SPIE Conference Proceedings, Vol. 718, 1986, pp 66-77.

8. S.A. Kingsley, "Fiber-Optic Sensors: Opportunities for Distributed Measurement," InTech, August 1985, pp 44-48.

9. J. Sirkis, "A Surface Application Technique for Optical-Fiber Strain Sensors," Experimental Techniques, November, 1988, pp 22-24.

10. B.Y. Kim, D. Park, and S.S. Choi, "Use of Polarization-Optical Time Domain Reflectometry for Observation of the Faraday Effect in Single-Mode Fibers," SPIE Conference Proceedings, Vol 718, 1986, pp 455-446.

11. Operating Manual for Millimeter Resolution OTDR System and Model TDR 10 Processing System, Opto-Electronics Inc., July 1987.

12. J. M. Senior, Optical Fiber Communications Principles

and Practice, copyright 1985, Prentice-Hall International, London, pp. 219-225.

13. "Optical Time Domain Reflectometry by Photon Counting," Electronics Letters, July 31, 1980, Vol. 16, No. 16, pp. 631.

14. C.G. Bethea, B.F. Levine, S. Cova, and G. Ripamonti, "High-Resolution and High-Sensitivity Optical Time Domain Reflectometer," Optics Letters, March 1988, Vol. 13, No. 3, pp. 233-235.

15. E.G. Popov, Introduction to mechanics of solids, copyright 1968, Prentice-Hall, Englewood Cliffs, NJ, pp 95, 102.

16. B. Culshaw, pp. 74-84.

17. C.M. Miller and S.C. Mettler, "A Loss Model for Parabolic-Profile Fiber Splices," The Bell System Technical Journal, Vol. 57, No. 9, November, 1978, pp. 3172.

18. I.A. White and S.C. Mettler, "Modal Analysis of Loss and Mode Mixing in Multimode Parabolic Index Splices," The Bell System Technical Journal, Vol. 62, No. 5, May-June 1983, pp. 1189-1207.

19. S.C. Mettler, "A General Characterization of Splice Loss for Multimode Optical Fibers," The Bell System Technical Journal, Vol. 58, No. 10, December 1979, pp. 2163-2182.

20. D. Gloge and E.A.J. Marcatili, "Multimode Theory of Grade-Core Fibers," The Bell System Technical Journal, Vol 52, No. 9, November 1973, pp. 1563-1578.

21. AMP Inc., "Designer's Guide to Fiber Optics," 1982, pp 56-58.

22. CRC Handbook of Chemistry and Physics, CRC Press, Inc., Boca Raton, FL, 1984-85 edition, pp. D-187.

VITA

Carl Peyton Jacobson was born on December 30, 1951, in Phoenix, Arizona. He graduated from Chandler High School in Chandler, Arizona, in 1969 and then went on to graduate from Arizona State University with a Bachelor of Science in Engineering Science degree in 1974. With the exception of a one-year stint at Westinghouse Oceanic Division in Vallejo, California, Mr Jacobson has worked in a civilian capacity as an engineer for the U.S. Navy since 1974. He is a licensed Professional Engineer in Mechanical Engineering in California and is currently employed by the Naval Sea Systems Command's Fiber Optics Program Office in Washington, DC. In 1988 he was selected as a Visiting Scholar to Virginia Polytechnic Institute and State University for the purpose of studying Fiber Optics. He received his Master of Science in Electrical Engineering degree in May, 1990.